PCCP

Accepted Manuscript

ROYAL SOCIETY OF CHEMISTRY

www.rsc.org/pccp

Plasmonic resonance of Ag nanoclusters diffused in soda lime glasses

Promod Kumar[1*], Mohan Chandra Mathpal[2*], Anand Kumar Tripathi[2], Jai Prakash[3], Arvind Agarwal[2], M. M. Ahmad[1], H. C. Swart[3]

[1]*Functional nanomaterials research laboratory, department of Physics, National Institute of Technology, Hazratbal, Srinagar-190006, India.*

[2]*Department of Physics, Motilal Nehru National Institute of Technology, Allahabad-211004, India.*

[3]*Department of Physics, University of the Free State, Bloemfontein, ZA9300, South Africa.*

***Corresponding authors;**

[1]Promod Kumar, Email: pkpmcm@gmail.com,talk2promodthakur@gmail.com

Tel: (O) - 0194-2422032, (Fax): 2101/ 2422032, 2420475

[2]Mohan Chandra Mathpal; Email: mohanatnpl@gmail.com.

Tel: +91-532-2271263, Fax: +91-532-2545342.

Abstract

Silver nanoclusters were prepared in a soda-lime glass matrix through the ion-exchange ($Ag^+ \leftrightarrow Na^+$) method followed by thermal annealing in air atmosphere. The nanoscale pattering of Ag nanoclusters embedded in soda lime glass matrix in air atmosphere at the different annealing temperatures have been investigated. During annealing the Ag^+ are reduced to Ag^0 and subsequently form silver nanoparticles inside the glass matrix. A blue shift of 20 nm has been observed as a function of post annealing temperature. The photoluminescence intensity is highest at annealing temperature of 500°C for 1h which continuously decreases as annealing temperature increases up 600°C. The presence of spherical nanoparticles with a maximum particle size of 7.2 nm has been observed after annealing at 600°C for 1hour, which is consistent with Mie theory based results.

Keywords: Structural; Nanoparticles; Surface Plasmon Resonance; Metal forming and shaping.

Introduction:

The field of plasmonics has been established as an interdisciplinary area of researcher coming from different background such as physics, chemistry and engineering strive to discover and exploit new and excited phenomena associated with surface plasmons. This fact is largely due to their advantage to manipulate light at the nanoscale by exploiting the interaction of light with metallic nanostructures which exhibits interesting surface plasmon resonance (SPR) phenomenon[1-2]. The plasmonic behavior of metallic nanostructures show enormous scientific interest due to their unique and unusual physicochemical properties and functionalities compared to their bulk counterparts. These properties make them attractive in various applications such as plasmonics[3-4], nanoelectronics[5-6], and biotechnology[7-8] and nanophotonics[9-10]. Particularly, nano-

sized silver clusters dispersed in a transparent dielectric matrix exhibit interesting localized surface plasmon resonance (LSPR) absorption usually observed in the visible region due to their coherent oscillation of conduction band electrons when excited by electromagnetic radiations[11-13]. The resonance frequency of noble metals, such as silver and gold falls in the visible and infrared region of the solar spectrum which attracts the scientific community to its solar photovoltaic applications. The electromagnetic coupling between metal nanoparticles is of essential importance in material science, which opens up a new horizon at nanoscale for advanced bio-molecule sensing, cancer treatment, plasmonic solar cell and various other practical applications. The plasmonic response of metallic nanoclusters can be tuned by controlling their size, shape, inter-particle separation, volume fraction of the metal nanoparticles and the dielectric constant of the embedding matrix, which gives a broad spectrum to scientific research in the field of plasmonics[14-15]. Plasmonic materials with large third-order optical nonlinearities and fast nonlinear response time are usually considered promising candidates for potential applications in optoelectronics, photovoltaic and photonic devices including flat screen TVs, electronic book readers, optical computing, optical data storage, all-optical switching devices, organic thin film transistors, organic photovoltaic devices, biosensors, optical telecommunications, solid state lighting but also in harmonic generation and photodynamic therapy[5,16]. Ultrafast all-optical switching devices generally act as key components for the next generation broadband optical networks[17]. In general, the major requirements of such devices demands plasmonic materials with low linear and non linear loss, good optical quality and mechanical stability, large third-order optical nonlinearities and ultra-short relaxation time and should be portable and affordable for the society. In this context, soda lime silicate glasses containing nanometer-sized clusters of noble metals are known to be most suitable and

promising materials due to their large third-order non linear susceptibility and ultrafast response properties[18,19]. Generally high efficient non linear optical materials based devices are expected to become a key components for high-capacity communications networks in which the ultrafast switching signal regeneration and high capacity optical recording media is required[18]. Due to its homogeneity, mechanical strength, high transparency, easy fabrication and solubility properties, soda-lime silicate glass matrices have been highly appreciated as an excellent host matrix for growing nano-sized metallic clusters. The metallic clusters can be nucleated by thermal treatment or radiation, and grow at a high temperature, resulting in a very narrow size distribution inside the soda-lime silicates glass matrix[5].

Soda-lime silicate glass embedded with silver nanoclusters can be synthesized by various methods such as, ion implantation, melt-quench technique, sol-gel methods, low energy ion-beam mixing, physical vapor deposition, ion exchange methods etc. Among these methods the ion exchange method has been considered one of the most important techniques to introduce metallic nanoclusters inside the glass surface because this technique is simple and does not require any sophisticated equipments. The ion exchange technique combines with thermal annealing has received an increase attention as it can be used to introduce metallic nanoclusters such as silver, gold and copper into soda-lime matrix[20]. Nano-sized Ag/Ag_2O nanoclusters on glass matrix have been found suitable candidates for potential applications in optical data storage[21-23]. In this work, the Ag nanoclusters dispersed in a soda-lime glass by ion-exchange method at 370°C followed by thermal annealing (in air) at various temperature for the nucleation and growth of Ag nanoclusters in soda-lime glasses have been investigated. The work provides an insight on nano-clustering and plasmonic effects of Ag nanoparticles embedded in soda-lime glass matrix.

Experimental

Nanoscale silver clusters were prepared in a soda-lime glass matrix through the silver ion-exchange ($Ag^+ \leftrightarrow Na^+$) process. Commercial soda lime glass (purchased from Blue Star Company, India) slides of 1 mm thickness (composition, weight %, 72.0% SiO_2, 14.0% Na_2O, 0.6% K_2O, 7.1% CaO, 4.0% MgO, 1.9% Al_2O_3, 0.1% Fe_2O_3, 0.3% SO_3) were first cleaned ultrasonically by using distilled water, trichloroethylene and acetone. Next, soda lime glass samples were dipped in a molten salt bath having 20 mol% $AgNO_3$ in $NaNO_3$ mixture heated to 370°C for 2 minutes in a crucible of Al_2O_3. It is important to note that the short time duration (2 minutes) was used for the exchange of ions. Under these conditions, the silver ions in a molten salt bath diffuse inside the glass matrix and replace the Na^+ by Ag^+ ions in the glass. After inter-diffusion the ion exchange samples were removed from molten bath and cleaned with distilled water and acetone to remove any silver nitrate adhering from the surface. The pristine samples were colorless or very faint yellow state. The change in optical properties occurs due to this inter diffusion in glasses because of different electrical polarisabilities of the exchanged ions, difference in their size (ionic radii) and mechanical stresses. These as-exchanged samples were annealed in air at various temperatures (500°C, 550°C and 600°C) for 1h to induce cluster growth inside the soda-lime glass matrix.

UV-visible absorption studies in the wavelength range of 300-800 nm were carried out on the samples using the dual beam spectrophotometer HITACHI U 3300. The soda lime glass was used as the reference for UV measurements. Photoluminescence studies were carried by the use of Flouromax Photoluminescence spectrophotometer. A JEOL JEM 2100 ultra high resolution field emission gun electron microscope (FEGTEM) operated at 200 kV was used to characterize the synthesized Ag ion exchange based annealed samples. Prior performing the FEGTEM

measurements the glass–metal nanocomposites slides (metal in glass matrices) were crushed to form the powder samples by using the pestle mortar. The few milligrams of obtained powder samples were dispersed in acetone and then the solution was kept in an ultrasonic bath for 45 minutes. The resulted suspension was pipetted from top portion of the liquid and few drops of the liquid were placed on a carbon coated copper grid of 300-mesh. The dispersed solution was then evaporated; the images were recorded using FEGTEM. XPS measurements were carried out the Perkin-Elmer PHI model using monochromatic Mg Ka radiation 1253.6 eV), produced by 15 KV electron impact on a magnesium anode at a power level of 300W and was used as an excitation source. To provide a resolution of 0.5 eV the pass energy was kept 25 eV. The photoelectron spectrometer work function was adjusted to get the Au $4f_{7/2}$ peak at 84eV.The binding energy of the core level photoelectron of Ag was conventionally calibrated by assuming the binding energy of the surface C-1s photoelectron to be 284.6 eV. Rutherford backscattering spectrometry (RBS) measurements were performed using 2 MeV He ions beams. The incident direction was normal to the sample surface, and scattered particles were detected at the angle of 165°C. In brief UV, PL, RBS, XPS and FEGTEM have been mainly utilized to understand the formation mechanism during thermal annealing in air, which is the key to optimize thermal processes for the nano-clustering and tuning the properties of silver nanoclusters inside the soda-lime glasses.

Results and discussion

Figure 1(a) show Rutherford backscattering spectra of as-exchanged and thermally treated soda-lime glass samples in air at various temperatures up to 600°C. The magnified image of Ag peak has been shown for clarity in Figure 1(b), which helps to understand the mechanism during the annealing process. It can be seen that at the surface, Ag concentration is higher in case of ion exchanged samples. After annealing, decrease in Ag peak height indicates the diffusion of Ag atoms in glass as can be observed in case when as-exchanged samples annealed at 500°C and 550°C.

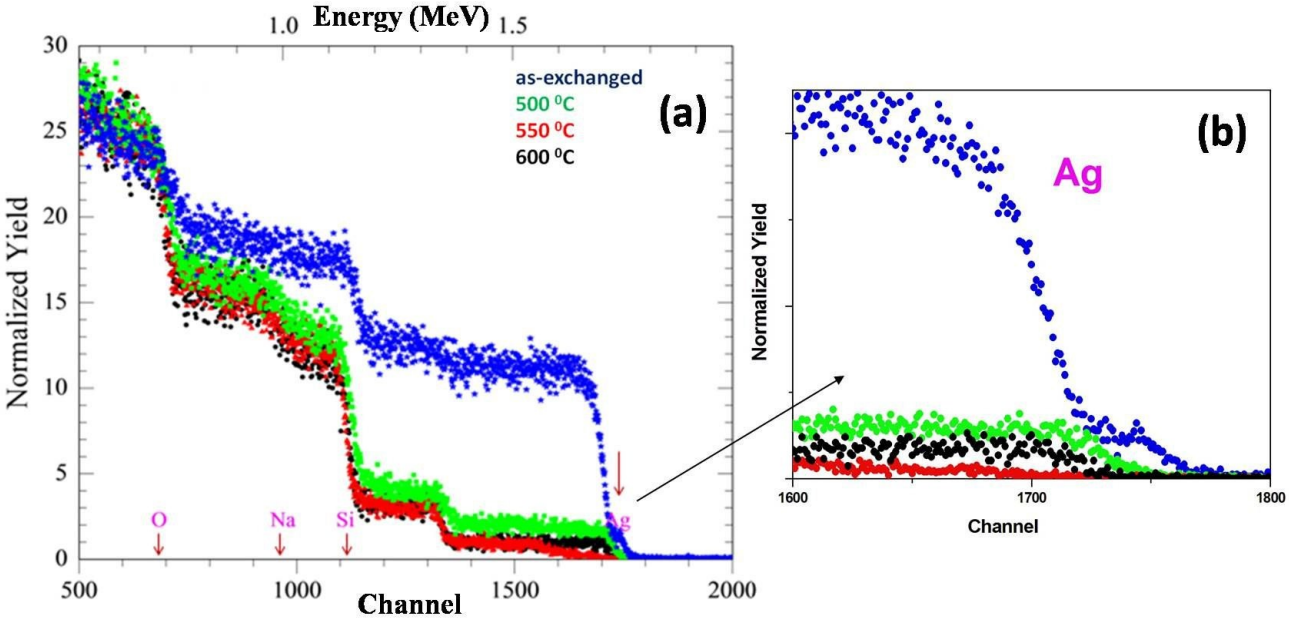

Figure 1: (a) RBS spectra of silver ion- exchanged glass (pristine) and annealed sample at various temperatures (500°C, 550°C and 600°C) for 1h and (b) magnified image of Ag peak has been shown for clarity.

It is observed from the Rutherford backscattering spectra that silver atoms accumulated near the surface of soda-lime glass during thermal annealing[24]. Accumulation of silver clusters is higher for the samples annealed at a temperature of 550°C for 1h. The near surface accumulation at

600ºC is observed between 500ºC and 550ºC. This may be due to the fact that more atoms are diffused in deep of the glass matrix, which results into the less surface accumulation at 600ºC. Although the surface accumulation is approximately same at 550ºC and 600ºC as the annealing at high temperatures (T≥ 550ºC) act as the nucleation center for the clusters. Therefore the annealing in air at various temperature confirms the silver diffusion into the soda–lime glass matrix which decreasing the near surface accumulation of silver ions as compared to the pristine sample. The surface accumulation results are similar to those seen from morphology observed in TEM images. Near surface accumulation is due to the thermal diffusion of silver ions in the soda-lime glass matrix. This outward diffusion of silver ions relaxes the stress (which arises due to the size differences of Ag^+ and Na^+ ions) and minimizes the total energy in the system[24].

Figure 2 show UV-visible absorption spectra of as-exchanged and thermally treated soda-lime glass samples in air at various temperatures (500°C, 550°C and 600°C) for 1 h. The optical macro images (photographs taken from camera) for the appearance of the samples are also shown in Figure 2 for their corresponding plot. The optical absorption spectra of as-exchanged Ag-doped glass samples does not show any SPR spectra indicating that the silver clusters formation did not occur, or the size of Ag nanoclusters were less than 1 nm in size during few min ion exchange at 370°C or ideally Ag^+ ion existed within the soda-lime glass matrix[25]. Annealing in air for 1h at 500°C, an absorption band was observed at 433 nm, which is apparently due to the localized surface plasmon resonance (LSPR) band of the silver nanoparticles inside the glass matrix. Annealing at still higher temperatures resulted in a blue shift in the LSPR peak to 413 nm. A significant blue shift of 20 nm (from 413 to 433 nm) of the LSPR peak has been observed in the sample annealed for 1h at 600°C. The intensity of the absorption peak increases with the increase of annealing temperature is attributed to the thermal

growth of the silver nanoclusters inside the glass matrix due to higher reduction of silver oxide. This is because more Ag^{+} ions were reduced into neutral Ag^{0} atoms, which indicates an increase of volume fraction of silver nanoclusters in the glass matrix[23]. The blue shift of LSPR peak was observed with increasing clusters size which lowers the value of full width at half maxima (FWHM) for increasing clusters size.

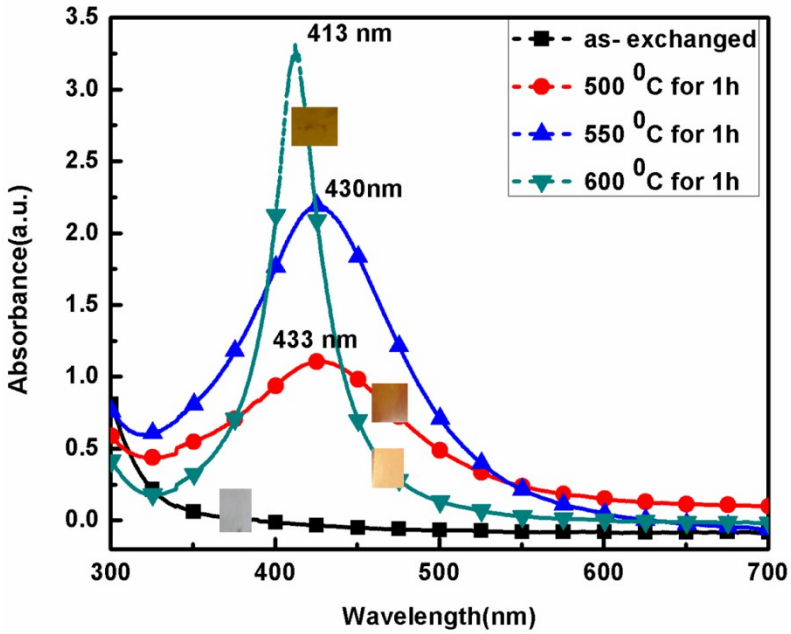

Figure 2: Optical absorption spectra with color photographs of thermal evolution of Ag nanocomposites glass.

For a small clusters (R ≤ 10 nm), this kind of decrease in FWHM with increase in clusters size is due to the mean free path effect of electrons[25]. In our case it is well known that the optical properties of Ag nanoclusters, which are homogenously dispersed in transparent glass matrix, depend on size-dependent permittivity $\varepsilon(\omega, R)$ of Ag nanoparticles and absorption extinction (K) of Ag nanoparticles, where $R \ll \lambda, and\ \lambda$ is the wavelength of light. It is explained by the following equations under the quasi-static or dipole-dipole approximation [26-27]:

$$\varepsilon(\omega, r) = \varepsilon_1(\omega) + \mathrm{i}\,\varepsilon_2(\omega, r)$$

$$= \quad \varepsilon_1(\omega) + i\left[\ \varepsilon_{2,bulk}\ (\omega) + \eta\ \frac{\omega_p^2}{\omega^3}\ \left(\frac{v_f}{r}\right)\right], \qquad (1)$$

$$K = \quad \frac{18\,\pi\,C\ \varepsilon_m^{3/2}(\omega)\ \varepsilon_2(\omega,r)}{\lambda\left[\{\varepsilon_1(\omega) + 2\,\varepsilon_m(\omega)\}^2 + \varepsilon_2^2(\omega,r)\right]} \qquad (2)$$

where ε_1 and ε_2 denote the real and imaginary components of the metallic nanoclusters dielectric constant of metal particles, respectively, $\varepsilon_m$is the dielectric constant of the surrounding medium (assumed to be frequency independent),ω_p is the Drude plasma frequency (for Ag, ω_p= 1.46 × 10^{16} s^{-1}), v_f = 1.39 × 10^6 m/s is the Fermi velocity for bulk silver and C is the volume concentration of the embedded particles; the parameter σ is the sum of two additive terms describing size and interface effects.

From eq. (2) it follows that resonance occurs when $\varepsilon_1(\omega)$= -2 ε_m, ie. the SPR condition. When this condition is fulfilled, the light field induces a resonant coherent oscillation of free electrons across the metal nanoparticle. The resonance condition is satisfied only for the noble metals such as Ag, Au and Cu nanoparticles at visible wavelengths. This is the origin of their intense color[26,28]. It was observed that the intensity of LSPR peak found around 433 nm increases significantly and the peak shifts to the lower wavelength side. The width of the absorption band reduces systematically with the increase in annealing temperature as shown in Figure 2. This indicates an increased volume fraction of Ag nanoclusters (growth of clusters) inside the silver ion exchanged glasses[28]. Assuming Drude- like the free particles behavior of electrons at nano-sized Ag particles, one can write,

$$R = \quad v_F\,\tau \qquad (3)$$

Where R is the average radius of the silver nanoclusters and τ is the mean free time (time between two successive collisions) of the conduction electrons at nano-sized metal particles. Spatial confinement and frequent scattering of conduction electrons over the silver nanoparticles

dispersed in a transparent glass matrix leads to quantum fluctuations (ΔE) of the average energy of the free electrons around the surface plasmon resonance. Therefore by applying the Heisenberg's uncertainty principle relation ($\Delta E.\Delta\tau = \hbar$), eq. (3) can be written as,

$$R = v_F \frac{\hbar}{\Delta E}$$

$$\text{or, } d = 2R = 2\frac{\hbar v_F}{\Delta E} \qquad (4)$$

where $\hbar$ *is* the Planck's constant and d is the average diameter of the silver nanoclusters. The energy-spread ΔE (in eV units) in eq. (4) has been estimated from the full width at half maximum (FWHM) of the optical absorption band. Eq. (4) is valid as long the size of silver clusters is much smaller than the mean free path of the electrons in the bulk metal. The mean free path of the electrons is about 27 nm at room temperature for bulk silver[9]. By using eq. (4), the Gaussian profile from UV-Vis spectra of Ag nanoparticles was plotted and estimated the average size of Ag nanoclusters to be 3, 3.9, 7 nm after annealing in air at various temperature (500°C, 550°C and 600°C) for 1h. These results show that the size of Ag nanoclusters increases with increasing annealing temperature due to the diffusion-limited aggregation of silver nanoclusters inside the soda-lime glass[29].

Table 1: Average clusters size estimated by using Mie theory at different annealing temperatures

Annealing temperature (°C)	Annealing time (h)	SPR wavelength (nm)	FWHM (eV)	Cluster size (nm)
500	1	433	0.60	3.0
550	1	430	0.47	3.9
600	1	413	0.26	7.0

In order to confirm the size of Ag nanoclusters embedded in glass substrate after annealing at different temperatures, transmission electron micrographs were taken from these samples. Figure 3, Figure 4 and Figure 5 show FEGTEM images for Ag ion exchange sample annealed at 500°C, 550°C and 600°C for 1h respectively. FEGTEM images show presence of spherical silver nanoparticles are embedded into the glass matrix at all the annealing temperatures. For plasmonic applications the dimension of nanoclusters is crucial. The average size of the nanoclusters estimated from the TEM images are found to be 2.9 nm, 4.4 nm and 7.2 nm for samples annealed at 500°C, 550°C and 600°C respectively for 1h (as shown in the histogram plot) which are in good agreement with the cluster size (shown in Table 1) calculated by equation (1). Analysis of high resolution TEM images for the sample annealed at 550°C and 600°C show that the spherical particles are consisted of crystal lattice with d-spacing of 0.24 nm, which corresponds to (111) plane of Ag nanoclusters. The selected area electron diffraction (SAED) pattern is also obtained for the sample annealed at 600°C indicates the presence of crystallographic plane (111) of Ag^0 clusters.

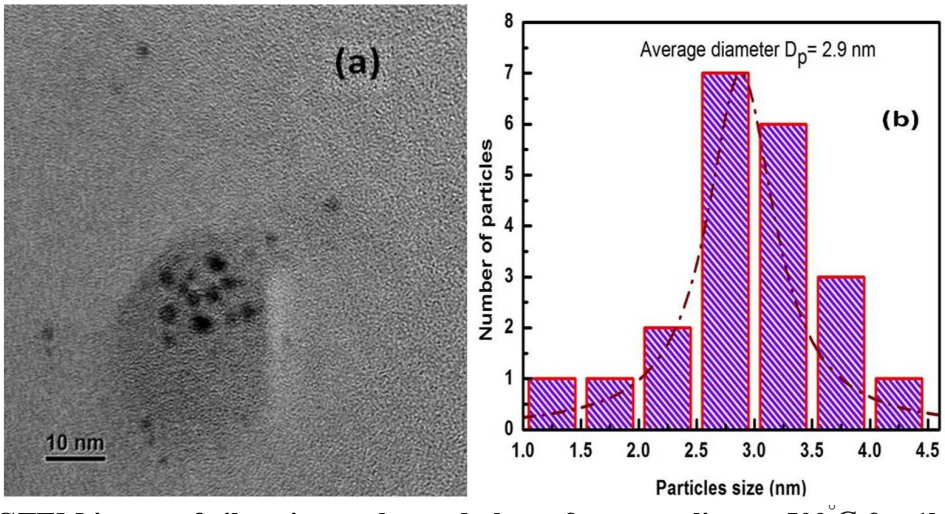

Figure 3: FEGTEM image of silver ion exchanged glass after annealing at 500°C for 1h. (a) at 10 nm scale and (b) particle size distribution curve.

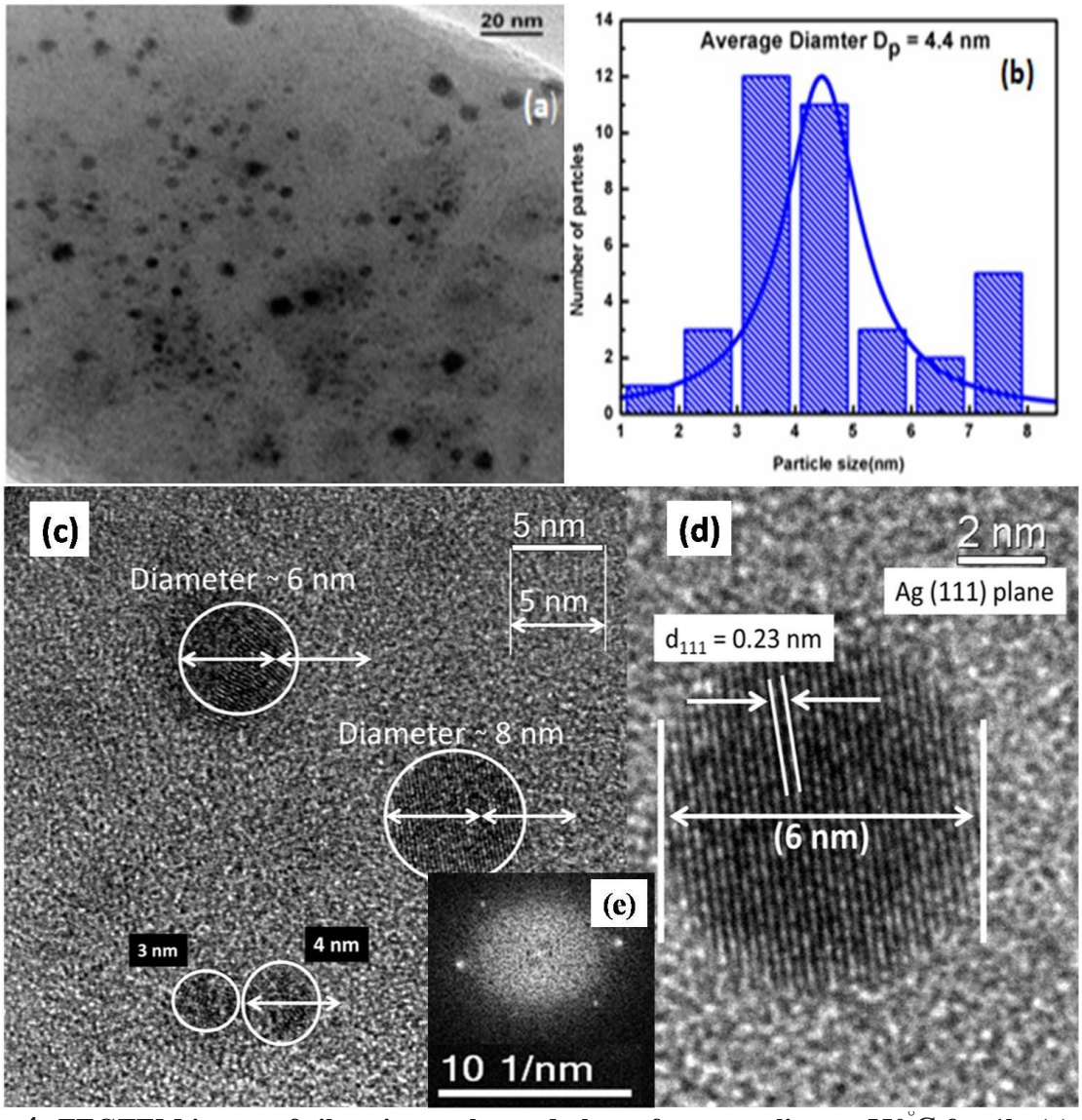

Figure 4: FEGTEM image of silver ion exchanged glass after annealing at 550°C for 1h. (a) at 20 nm scale, (b) particle size distribution curve, (c) at 5 nm scale, (d) at 2 nm scale and (e) Fast Fourier Transform (FFT) image.

Figure 6 shows the room temperature photoluminescence spectra of Ag^+- Na^+ ion exchanged soda lime glass after annealing at various temperatures (500°C, 550°C and 600°C) for 1h. At the excitation wavelength of 325 nm, the photoluminescence spectra of Ag exchanged soda lime glass show drastic changes in PL intensity after annealing at various temperatures (500°C, 550°C and 600°C) for 1h.

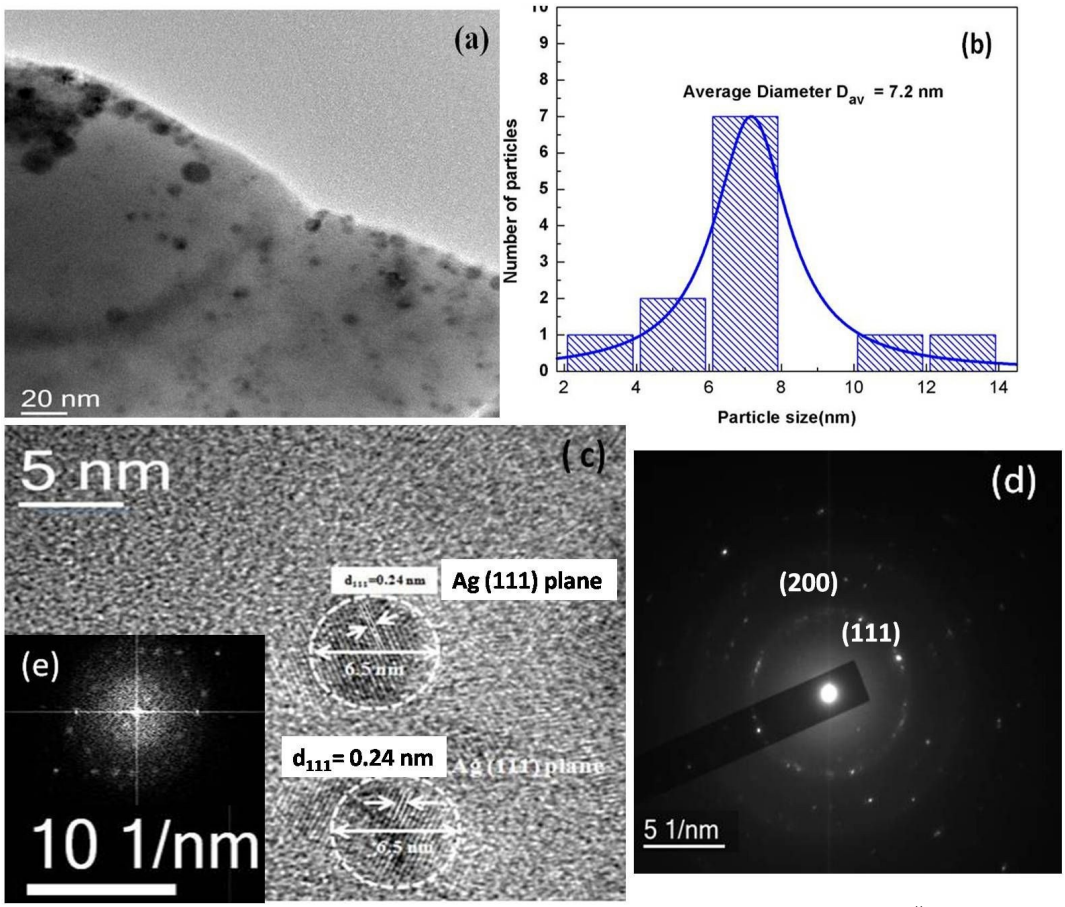

Figure 5: FEGTEM image of silver ion exchanged glass after annealing at 600°C for 1h. (a) at 20 nm scale, (b) particle size distribution curve, (c) at 5 nm scale, (d) SAED pattern and (e) FFT image.

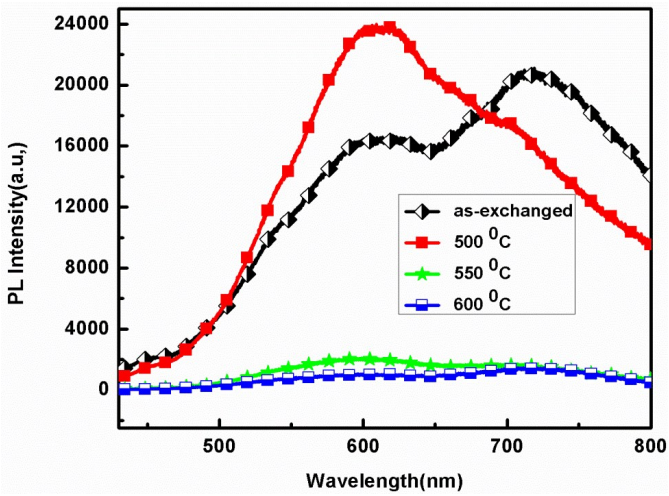

Figure 6: PL Spectra of silver ion-exchanged glass after annealing at various temperatures (500°C, 550°C and 600°C) for 1h.

It is clear from the figure that the PL intensity has maximum at 500°C, but when annealing temperature is increased further up to 550°C, PL intensity decreases drastically and has minimum value at 600°C. Villegas et al. has already reported that Ag^+ ions are luminescent in nature in both crystalline and glassy matrices[30].

In contrast, till now no PL emission was observed for Ag^0 (neutral atoms) at any excitation wavelength to the best of our knowledge. In addition to this the increase in PL intensity at an annealing temperature of 500°C for 1 h could be due to the increase of volume fraction of Ag^+ ions in the bulk soda lime glass matrix. The decrease in PL intensity with further ion exchange at higher temperature and/or thermal annealing of ion exchanged glass results in reduction of Ag^+ ions leading to increased formation of Ag^0 atoms. Further increase in annealing temperature leads to the rapid growth of silver nanoparticles and that might have resulted in the quenching of PL intensity for the samples annealed at 550°C and 600°C for 1h[8,31]. P. Gangopadhyay et al. has reported similar results for silver nanoclusters in ion exchanged soda lime glass followed by thermal annealing in vacuum[32]. Simo et al. reported that the PL intensity of the ion-exchanged (Na^+-Ag^+) sample is increases with increase in molecular clustering, which were formed during annealing below the threshold temperature (410°C)[23]. Annealing below the threshold value leads to the selective formation of clusters (d<1 nm) which are most likely silver dimmers. With increasing annealing duration only the number of clusters increases. After longer annealing durations the PL intensity decreases and vanishes after annealing at 550°C due to a decrease of cluster concentration[23].

Figure 7 shows the Ag -3d XPS spectrum of as exchanged and silver ion exchanged glass sample annealed in air at 550°C. An XPS survey spectrum of the cluster clearly shows the

presence of the expected elements, C, O, Ag, and Na as shown in Figure 7 (a). The adventitious carbon is expected due to natural contamination from atmosphere and evacuation problems in vacuum chamber of XPS instrument. The XPS spectrum of as-exchanged Ag-doped glass sample is also shown for comparison. The binding energy of as-exchanged samples has been found 367.65 eV in the Ag-$3d_{5/2}$ peak which gives the signature of Ag/Ag_2O exist inside the Ag-ion exchanged soda-lime glass. The annealed film illustrates spin–orbit splitting of the Ag-3d levels, manifested as Ag $3d_{3/2}$ and Ag $3d_{5/2}$ respectively as shown in Figure 7 (b). The core level spectra of annealed sample show Ag-$3d_{3/2}$ (~374.0 eV), Ag-$3d_{5/2}$ (~368.0 eV) positions indicating the presence of silver in metallic form in the glass matrix and the difference between two Ag peaks is 6.0 eV. The binding energy position which appears at 368.0 eV for the Ag $3d_{5/2}$ peak gives the signature of Ag^0 pure metallic atom inside the glass matrix. In an earlier studiy[33] it was observed that, the chemical states of Ag in TiO_2 samples exist mainly as Ag^0 (metallic Ag) and Ag^+, associated with the Ag-$3d_{5/2}$ XPS signals at 368.2 (in our case 368.0) and 370.3 eV (in our case 367.6 eV)[33] respectively. The C-1s peaks appearing at 284.6 (Pristine) and 284.8 eV (at 550°C) are assigned to C in –COO, C–C as shown in Figure 7(c). Figure 7(d) shows the O-1s core-level emission corresponding to the pristine and annealed sample in air at 550°C for 1h. O-1s spectra for the pristine sample appear 531.6 eV, while the annealed sample occurs at 531.8 eV, which can attribute to the presence of SiO_2 in glass matrix. In some studies it was observed that, the chemical states of Ag associated with the Ag $3d_{5/2}$ in Ag-doped semiconducting samples exist as Ag^0 (metallic Ag) at 367.9, 368.1 or 368.2 eV, Ag^{2+} (AgO phase) at 367.0 or 367.8 eV and Ag^+ (Ag_2O phase) at 367.6, 367.4 or 367.7 eV in XPS signals respectively[34-40]. Therefore the XPS results indicate that the silver is present in the form of silver oxide completely in the pristine sample. The Ag $3d_{5/2}$ peak broadening for the sample annealed at 550°C shows that silver is also

partially present in the form of Ag^{+} for the formation of silver oxide (AgO/Ag_2O phase)[36-40]. Durucan and Akkopru have also reported that metal oxides are highly unstable at higher temperatures and decompose into pure metal nanoparticles in air at temperatures higher than 500°C[40]. In this work this complete conversion of silver oxide to metallic silver is observed only after an annealing temperature of higher than 550°C, which may be due to the fact of higher concentrations of Ag based nanoclusters. Recently it has also been observed that low concentration of Ag loading does not respond to the XPS signals in the pristine samples[37].

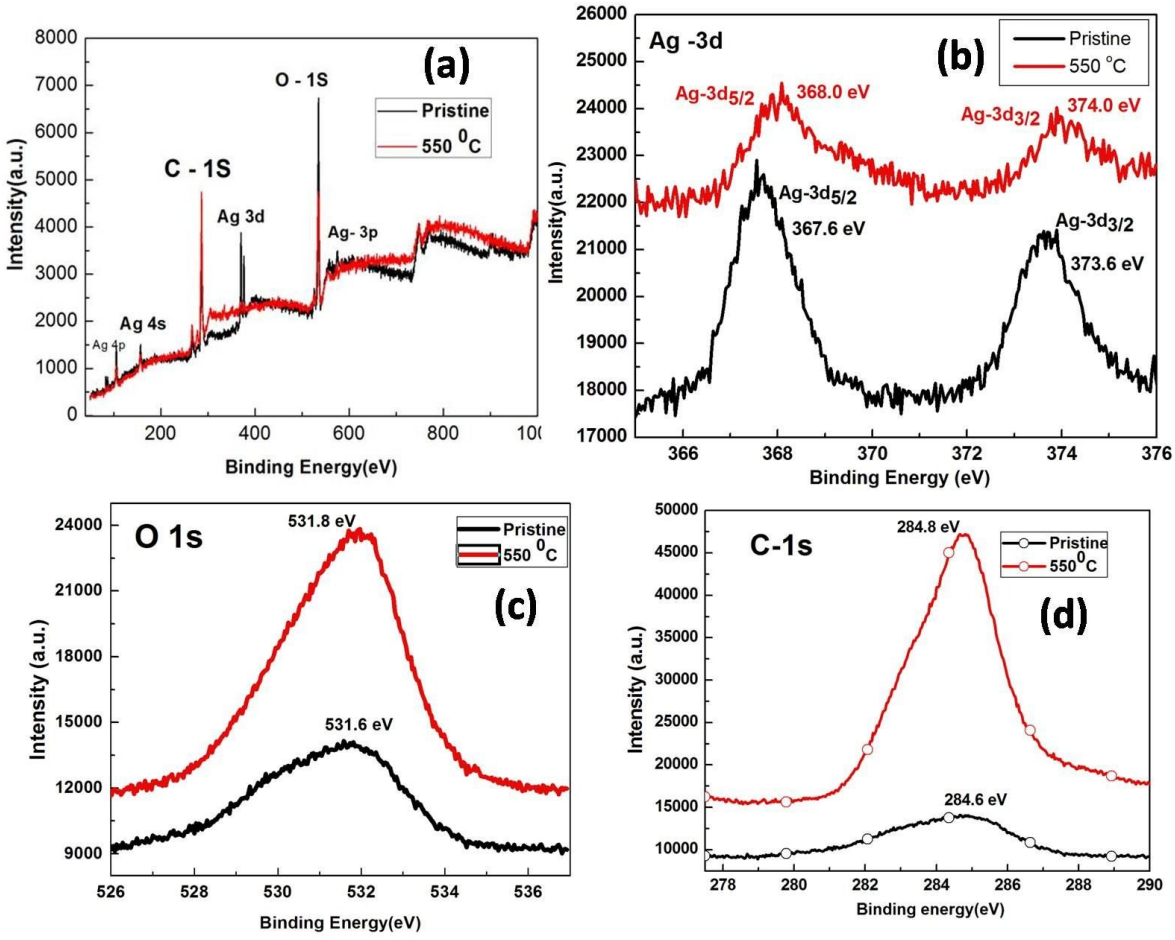

Figure 7: XPS spectrum of the Ag nanoclusters in ion exchanged glass (pristine) and annealed sample at 550°C: (a) general scan spectra, (b) silver (Ag) core level spectra, (c) carbon (C) core level spectra and (d) oxygen (O) core level spectra.

Based on UV, PL and XPS results the silver oxide completely converts into metallic Ag for the sample annealed at 600°C as it is highly reducible at a temperature higher than 500°C[38-40].

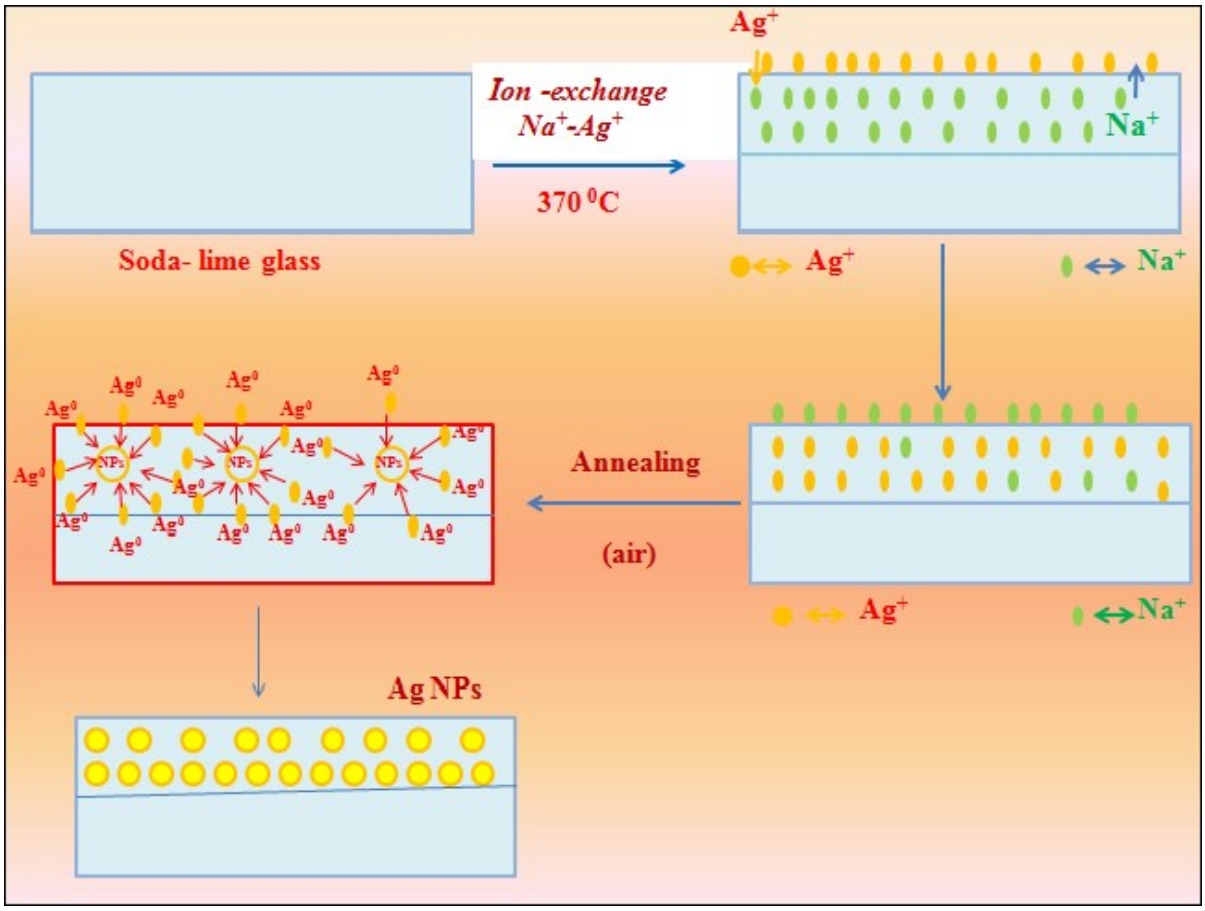

Figure 8: Schematic diagram depicting thermal evolution of Ag nanoclusters in an ion exchanged soda- lime glass.

The formation mechanism of Ag nanoclusters in ion exchanged glass followed by thermal annealing in air could be understood as follows as shown in Figure 8. Ion exchange at 370°C leads to incorporation of Ag atoms into soda-lime glass matrix after substituting the Na atoms of glass matrix. These Ag atoms in ion exchanged glass exist mainly in the form of Ag^+ ions along with a small population of Ag^0 atoms[31]. As the annealing temperature increases it results in further reduction of Ag^+ ions after capturing the electrons from the glass matrix or from the impurities leading to increased formation of silver neutral atom (Ag^0)[30]. The increase in

annealing time and temperatures further increases the formation of more silver (Ag^0) neutral atom. The silver atoms (Ag^0) are mainly bound to non-bridging oxygen (NBO) in glass matrix. Ag-O bonds break during thermal annealing to form more Si-O and Ag-Ag bonds. Hence Ag^0 become a dominate state. The ionic size difference between Ag^+ and Na^+ leads to tensile stress in the surface region of silver ion-exchange ($Ag^+ \leftrightarrow Na^+$) soda-lime glass. During annealing Ag atoms diffuse towards the soda-lime glass surface for thermal relaxation of the surface tensile stress due to the size difference after cooling[31,38]. This relaxation and precipitation of Ag atoms leads to the formation of Ag nanoclusters inside the glass matrix. Thermal treatment in oxidizing atmosphere leads to diffusion of oxygen atoms also into the near-surface metal-doped layer in the soda lime glass, which results into the oxidation of Ag nanoclusters in the form of Ag/Ag_2O nanoparticles. Since the diffusion of Ag inside the soda-lime glass matrix is nominal, the above discussed processes of silver nanoclusters formation are commonly carried out through thermal treatment in air. When electromagnetic radiation interacts with these nano-sized metal/metal-oxide particles which are much smaller than the wavelength, its conduction electrons could be displaced from their nuclei. Hence, opposite charges will be build up on the metal nano particle's surface which acts as a restoring force for the oscillating electrons. Such oscillations are maximized when the frequency of the incoming light matches the inherent oscillating frequency of the fluctuating conduction electrons which is responsible for plasmon resonance.

Conclusions

The synthesis of Ag nanoclusters embedded in soda lime glass by Na^+-Ag^+ ion exchange followed by thermal annealing in air has been performed. It demonstrate that ion exchanged Ag nanoparticles diffuses in pure soda glass matrix during annealing processes. After annealing at higher temperature these particles are reduced to neutral silver atom (Ag^0) and subsequently

form silver nanoparticles in air (open) atmosphere. The luminescence intensity of thermally exchanged samples decreases with increase in annealing time and temperature. Photoluminescence, UV, RBS and XPS spectra confirm clustering and precipitation of Ag atoms leads to the formation of Ag nanoclusters with increase in annealing temperature. TEM image shows the presence of spherical nanoparticles with the average cluster size, which agrees with the average cluster size calculated by UV-Visible absorption spectroscopy.

Acknowledgement:

The authors are highly thankful to Prof. (Dr) Rajat Gupta (Director NIT Srinagar) and Fayaz Ahmad Mir (Registrar NIT Srinagar) for taking keen interest in research and extending financial support for carrying out the research work. One of the Author Mr. Promod kumar is also thankful to Shri P. L. Sapporo (PA to Director) of NIT, Srinagar for his generous help and support in administrative understandings.

References:

[1] M. Giloan, S. Zaiba, G. Vitrant , P.L. Baldeck , S. Astilean, *Optics Communications*, 2011, **284**, 3629–3634.

[2] W.L. Barnes, A. Dereux, T.W. Ebbesen, *Nature,* 2003, **424**, 824.

[3] S.A. Maier, P.G. Kik, H.A. Atwater, *Appl. Phys. Lett.* 2002, **81**, 1714–1716.

[4] S. Pillai, K.R. Catchpole, T. Trupke, M.A. Green, *J. Appl. Phys*. 2007, **101**, 093105.

[5] Anne Simo, Jorg Polte, Norbert Pfander, Ulla Vainio,Franziska Emmerling, and Klaus Rademann, *J. Am. Chem. Soc.* 2012, **134**, 18824−18833.

[6] B. Mukherjee, M. Mukherjee, *Appl. Phys. Lett*., 2009, **94**, 173510.

[7] A. Kumar, P.K. Vemula, P.M. Ajayan, G. John. *Nat. Mater.* 2008, **7**, 236–241.

[8] J.C. Riboh et al., *J. Phys. Chem. B*, 2003, **107**, 1772–1780.

[9] E. Heolweil and R.M. Hochestrasser, *J. Chem. Phys.* 1985, **82**, 4762-4770.

[10] Y. Dirix, C. Bastiaansen, W. Caseri, and P. Smith, *Adv. Mater.* 1999, **11**, 223-227.

[11] V. Amendola, O.M. Bakr, F. Stellacci, *Plasmonics*, 2010, **5**, 85.

[12] X.M. Zhang, J.J. Han, Q. Zhang, F.F. Qin, J.J. Xiao, *Optics Communications*, 2014, **325**, 9–14.

[13] J. S. Sekhon, S. Verma, *Plasmonics,* 2011, **6**, 163.

[14] S. Ju, V. L. Nguyen et al.,*J. Nanosci. Nanotechnol.* 2006, **6**, 3555-3558.

[15] K. L. Kelly, E. Coronado, L. L. Zhao, G. C. Schatz, *J. Phys. Chem. B,* 2003, **107**, 668– 677.

[16] A. Zewadzka, P. Plociennik, J. Strezelecki, A. Korcala, A.K.Arof, B.Sahraoui, *Dyes and Pigments,* 2014, **101**, 212-220.

[17] Yang Xiu Chun, L.I Zhi Hui, L. I Weijie, XU JingXian, Dong Zhi Wei & Qian Shi X. Siong, *Chinese Bulletin Science*, 2008, **53(5)**, 695-699.

[18] R. Philip, G. Ravindra Kumar, N. Sandhyarani, et al., *Phys. Rev. B*, 2000, **62**, 13160.

[19] G. Battaglin, P. Calvelli, E. Cattaruzza, et al., *Appl. Phys. Lett.* 2001, **78**, 3953.

[20] Khaled Farah, Faouzi Hosni, Arbi Mejri, Bruno Boizot, Ahmed Hichem Hamzaoui, Hafedh Ben Ouada, *Nuclear Instruments, and Method in Physics Research B,* 2014, **323**, 36-41.

[21] L.A.Peyser, A.E.Vinson, A.P.Bartko, R.M.Dickson, *Science,* 2001, **291**, 103.

[22] Christ Strohhofer, Jacob P. Hoogenboom, Alfons van Blaaderen, and Albert Polman. *Advanced Materials*, DOI: 10.1002/adma.200290007.

[23] Anne Simo, Jörg Polte, Norbert Pfänder, Ulla Vainio, Franziska Emmerling, and Klaus Rademann, *J. Am. Chem. Soc.* 2012, **134**, 18824−18833.

[24] E. Borsella et al., *Journal of Non-Crystalline Solids,* 1999, **245**, 122-128.

[25] P. Manikandan et al., *Spectrochimica Acta Part A: Molecular and Biomolecular Spectroscopy,* 2014, **124**, 203-207.

[26] Kreibig U, Vollmer M (1995) Optical properties of metal clusters. *Springer,* New York.

[27] Manish Kumar & C. S. Suchand Sandeep & G. Kumar & Y. K. Mishra & R. Philip & G. B. Reddy, *Plasmonics,* 9, **2014**, 129–136.

[28] Hutter, E., and Fendler, J. H., *Adv. Mater.* 2004, **16**, 1685.

[29] Chen et al., *Materials Research Bulletin,* 2013, **48**, 4667–4672.

[30] M. A. Villegas., *J. Sol-Gel Sci. Technol.* 1998, **11**, 251.

[31] P. W. Wang, *Appl Surf Sci*, 1997,**120**, 291–8.

[32] Gangopadhyay et al., *Phys. Rev. Lett.* 2005, **94**, 047403.

[33] Zhiyue Han , Jingchang Zhang , Yue Yu , Weiliang Cao, *Materials Letters*, 2012, **70**, 193–196.

[34] M. A. Garcia, M. G. Heras, E. Cano, J. M. Bastidas, M. A. Villegas, E. Montero, J. Llopis, C. Sada, G. D. Marchi, G. Battaglin, P. Mazzoldi, *J. Appl. Phys.*, 2004, **96 (7)**, 3737-3741.

[35] K. Xu, J. Heo, W. J. Chung, *International Journal of Applied Glass Science*, 2011, **2(3)**, 157–161.

[36] C. D. Wagner, W. M. Riggs, L. E. Davis, J. F. Moulder, handbook of X-ray photoelectron spectroscopy. Published by Perkin-Elmer Corporation, physical electronics division, 1979.

[37] M. C. Mathpal, P. Kumar, S. Kumar, A. K. Tripathi, M. K. Singh, J. Prakash, A. Agarwal, *RSC Advances***,** 2015, **5**, 12555-12562.

[38] J. Sheng, *International Journal of Hydrogen energy*, 2009, **34**, 2471-2474.

[39] M. Ferraris, S. Ferraris, M. Miola, S. Perero, C. Balagna, E. Verne, G. Gautier, C. Manfredotti, A. Battiato, E. Vittone, G. Speranza, I. Bogdanovic, *J Nanopart Res,* 2012, **14,** 1287-1306.

[40] C. Durucan, B. Akkopru, *Journal of Biomedical Materials Research B: Applied Biomaterials,* 2010, **93B**, 448-458.